How to cite: *Angew. Chem. Int. Ed.* **2020**, *59*, 23329–23334
International Edition: doi.org/10.1002/anie.202006874
German Edition: doi.org/10.1002/ange.202006874

Covalent Patterning

Covalent 2D-Engineering of Graphene by Spatially Resolved Laser Writing/Reading/Erasing

*Konstantin Felix Edelthalhammer, Daniela Dasler, Lisa Jurkiewicz, Tamara Nagel, Sabrin Al-Fogra, Frank Hauke, and Andreas Hirsch**

Abstract: *We report a facile and efficient method for the covalent 2D-patterning of monolayer graphene via laser irradiation. We utilized the photo-cleavage of dibenzoylperoxide (DBPO) and optimized the subsequent radical additions to non-activated graphene up to that level where controlled covalent 2D-patterning of graphene initiated by spatially resolved laser writing is possible. The covalent 2D-functionalization of graphene, which is monitored by scanning Raman microscopy (SRM) is completely reversible. This new concept enables write/read/erase control over the covalent chemical information stored on the graphene surface.*

Introduction

Research into the 2D carbon allotrope graphene has been a challenging topic spanning physics, chemistry and materials science since its discovery in 2004.[1–3] The chemical functionalization of graphene plays a fundamental role in modifying the outstanding properties of this atomically thin all carbon architecture. For this purpose, first prototype concepts of both covalent and non-covalent functionalization of graphene have been developed in recent years.[4,5] The covalent modification is accompanied by the introduction of sp^3 centers carrying the chemically bound addends. In this regard, additions of in situ generated radicals has been demonstrated to proceed rather facile.[6] Prominent examples are radical additions initiated by the reductive decomposition of diazonium salts,[7,8] iodonium salts,[9–12] aryl-, and alkylhalides.[13–15] This reaction type can be further facilitated by reductive alkali metal activation of graphite (metal intercalation) or of graphene supported on substrates.[12,15–21] The first steps towards this endeavor constituted a random and locally uncontrolled functionalization.[22,23] The next exciting challenge is the specific tailoring of covalent functionalization to confined graphene regions leading to controlled graphene patterning with covalently bound addends (2D chemistry of graphene). The spatial controlled patterning of functional moieties onto monolayer graphene presents the possibility of combining several unique properties, like region specific hydrophilicity-hydrophobicity, catalytically or optically active domains, anchoring group reservoirs for molecular recognition and patterned electron conductivity. This allows for the generation of materials, surfaces and devices engineered for specific demands. So far, some first approaches towards 2D-patterning of graphene relied on the implementation of masks consisting of poly(-methyl methacrylate) (PMMA) and subsequent lithography to access graphene for covalent functionalization in predefined regions. For the corresponding covalent functionalization Diels–Alder reactions,[24] hydrogenations and reactions with diazonium ions have been applied.[25] The drawback of the initial studies is the comparatively low degree of functionalization as indicated by low I_D/I_G ratios in the Raman spectra. We have recently considerably improved the field of covalent 2D-patterning of graphene by a) combining the mask assisted 2D-patterning with the reductive activation of graphene *prior* to the covalent addend[26] and b) by establishing a spatially resolved bottom side fluorination of graphene.[27] Although these improvements are very important, alternative concepts avoiding the implication of mask-assisted or other types of pre-patterning methods are highly welcome. The photochemical reactivity of graphene towards peroxides opening the opportunity of laser writing represents an attractive approach for this task.[28]

Herein, we report a facile and efficient method for the covalent 2D-patterning of monolayer graphene via laser irradiation affording high degrees of functionalization. We utilized the photo-cleavage of dibenzoylperoxide (DBPO) and optimized the subsequent radical additions to non-activated graphene up to that level where controlled covalent 2D-patterning of graphene initiated by spatially resolved laser writing is possible. Furthermore, the covalent 2D-functionalization of graphene is completely reversible, enabling a write/read/erase control over the covalent chemical information stored on the graphene surface.

Results and Discussion

Our approach towards a mask-less locally controlled functionalization utilizes the generation of reactive aryl

[*] K. F. Edelthalhammer, D. Dasler, L. Jurkiewicz, T. Nagel, S. Al-Fogra, Dr. F. Hauke, Prof. Dr. A. Hirsch
Department of Chemistry and Pharmacy & Joint Institute of Advance Materials and Processes (ZMP), Friedrich-Alexander University of Erlangen-Nürnberg
Nikolaus-Fiebiger-Strasse 10, 91058 Erlangen (Germany)
E-mail: andreas.hirsch@fau.de
Supporting information and the ORCID identification number(s) for the author(s) of this article can be found under: https://doi.org/10.1002/anie.202006874.

© 2020 The Authors. Published by Wiley-VCH GmbH. This is an open access article under the terms of the Creative Commons Attribution Non-Commercial NoDerivs License, which permits use and distribution in any medium, provided the original work is properly cited, the use is non-commercial, and no modifications or adaptations are made.

radicals generated from DBPO deposited onto the graphene monolayer. The oxygen-oxygen bond in DBPO is rather weak and therefore can undergo homolysis resulting in the formation of two benzoyloxyl radicals. Subsequent decarboxylation of the benzoyloxyl radicals leads to the generation of two phenyl radicals.[29,30] The decomposition of DBPO is initiated by either photolytic or thermolytic cleavage of the peroxide bond. For our 2D-patterning we induced the homolytic cleavage of the DBPO by irradiation with a 532 nm laser (Scheme 1b).[28] The created phenyl radicals undergo covalent topside binding to graphene. Solely supratopic binding, however, would create a huge amount of strain energy and unrealistic bending of the graphene lattice.[22] In our cases this is compensated by antaratopic back bonding of substrate functionalities quenching the initially formed radical centers on graphene and allowing for the establishment of strain free environments.[22,27,31,32] Here, Si/SiO_2 as a substrate plays an important role as it allows for the antaratopic backside bonding through its functional groups, relieving strain.

For the laser induced binding of phenyl radicals to graphene DBPO was dissolved in diethyl ether and one drop of the 10^{-3} M solution was placed on top of monolayer graphene deposited on a Si/SiO_2 substrate (for experimental details see electronic supplementary information ESI). After evaporation of the diethyl ether at room temperature, a thin, crystalline film of DBPO formed on the graphene surface (Figure S1). This DBPO film is the fundamental starting point for our locally controlled functionalization of the graphene layer beneath. By laser irradiation, the peroxide bond is cleaved homolytically and after extrusion of CO_2 reactive phenyl radicals are formed. The radicals are only formed in those areas where the laser hits the DBPO film resulting in a locally controlled addend binding accompanied by the generation of sp^3 carbon defects. In accordance to the work of Brus et al.[28] we have chosen a green laser (532 nm) for the photoexcitation of the peroxide film. As can be seen in Figure 1, a 60 second (0.88 mW, laser spot size $\approx 1\ \mu m^2$) irradiation of the film-covered graphene sample clearly results in a significant increase of the D-band intensity, indicative for the covalent binding of photo-generated phenyl radicals.

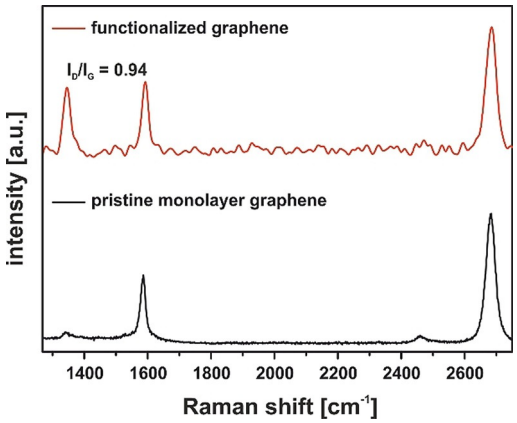

Figure 1. Raman spectrum of the pristine monolayer graphene on Si/SiO_2 (black) and Raman spectrum after illumination of the DBPO film for 60 seconds (red). $\lambda_{exec.} = 532$ nm, 0.88 mW.

In principle, the laser based covalent "writing" of functional entities on graphene cannot fully be decoupled from an additional radical generation/graphene functionalization attributed to a laser based Raman read-out of the "written" information. Therefore, we have investigated the contribution to the respective I_D/I_G ratios of our chosen standard "reading"

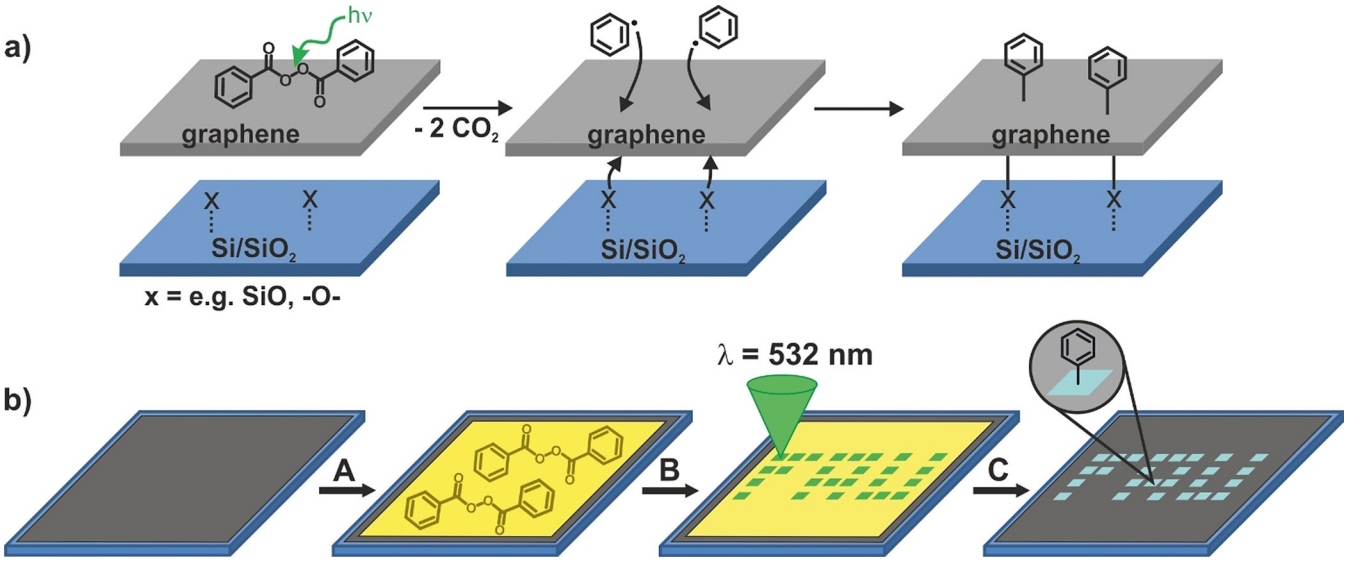

Scheme 1. a) Mechanism of the laser induced functionalization of graphene with DBPO, which involves antaratopic back bonding of the Si/SiO_2 substrate. b) Laser patterning of graphene on Si/SiO_2 by spatially controlled cleavage of DBPO: A) Drop casting of DBPO dissolved in diethyl ether leading to a DBPO coating on top of the graphene monolayer; B) Laser irradiation with a 532 nm laser of locally predefined areas and subsequent functionalization of the monolayer graphene by the laser-generated reactive radical intermediates; C) Removal of the residual crystalline DBPO coating by washing with acetone.

© 2020 The Authors. Published by Wiley-VCH GmbH

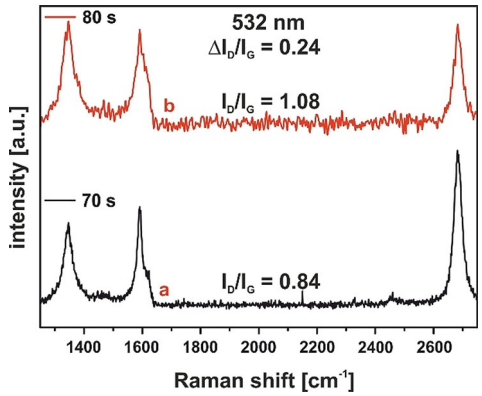

Figure 2. Black: Raman measurement of DBPO coated graphene after laser irradiation of 70 s. Red: Raman measurement of the same spot with an additional 10 s laser irradiation showing the I_D/I_G increase due to the read-out measurements.

conditions (0,88 mW, integration time: 10 s) to the initial I_D/I_G ratio of the writing process (Figure 2).

Here, the peroxide covered sample was irradiated for 70 seconds at the same laser spot, resulting in an I_D/I_G ratio of the writing process of 0.84. Subsequently, the same spot was irradiated for another 10 seconds to simulate the standard Raman reading conditions. As can be seen the additionally applied laser time leads to a subsequent increase of the initial I_D/I_G ratio of about 0.24. It has to be kept in mind, that this additional functionalization becomes less dominant the longer the initial laser writing time and therefore the achieved degree of functionalization has been chosen. Furthermore, a continues laser irradiation of the sample over a certain time span yields a very similar I_D/I_G ratio as can be achieved for iterative sample irradiations summing up to the same time span (Figure S2). These results nicely contribute to our picture that a laser based covalent writing of functional moieties on graphene is in an easy and highly efficient way possible by our chosen approach.

The next step was the determination of the most suitable parameters for the photo-generation of the intermediate aryl-radicals and their subsequent efficient binding to the graphene lattice. For this purpose, we carried out a systematic study, analyzing the influence of the laser intensity and irradiation time of a 532 nm laser on the degree of functionalization. In a first experiment, we selected a specific irradiation spot on the graphene surface and varied the irradiation time from 30 seconds to 16 minutes (30 s, 60 s, 120 s,…). It has to be kept in mind that for the read-out of the written information additional Raman measurements of 10 second laser irradiation has been carried out for each data point, extending the over-all irradiation time of the sample to 40 s, 80 s, 150 s … (Figure 3, individual spectral information presented in Figure S3). As discussed before, for the read-out process an additional contribution of about 0.24 to the respective I_D/I_G ratio has to be expected—affecting to a higher degree the data points obtained for shorter irradiation time spans.

The time study revealed that already irradiating for one minute leads to a significant increase of the D-band intensity,

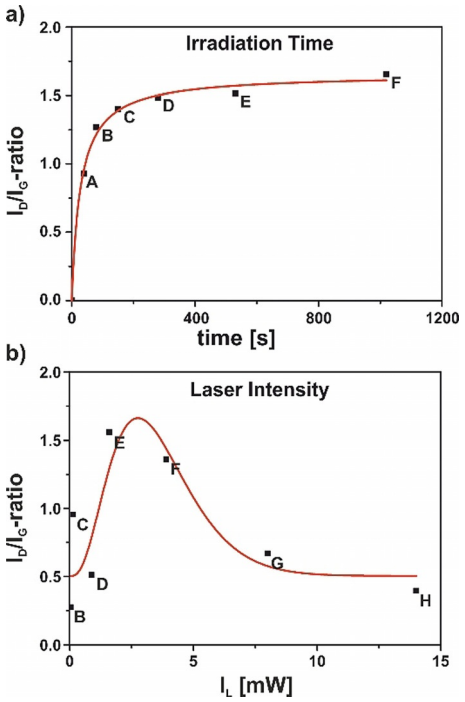

Figure 3. Evolution of the I_D/I_G ratios for the a) irradiation-time study ranging from 30 seconds up to 16 minutes and the b) laser-intensity study with laser powers of 0.017 mW to 14 mW—the individual Raman spectra are depicted in Figure S3 and S4 in the Supporting Information.

which correlates with an increase of addend carrying sp^3 centers. After two minutes, the D-band did not increase any further indicating that all of the DBPO present at the irradiated area decayed to the aryl radicals resulting in a saturation of addend binding (Figure 3a).

In a second experiment we have varied the laser intensity from 0.017 mW to 14 mW applied for a fixed time span of one minute. In contrast to the experiment described above, we have here changed the measuring spots on the sample after each individual measurement. As the analysis of the obtained spectral information shows (Figure 3b), the most intense D-band emerges after an irradiation with 1.6 mW laser intensity. At higher intensities of 4 mW and above a decrease in D-band intensity can be detected (respective Raman spectra are depicted in Figure S4) due to the fact that the energy introduced to the system at these intensities already leads to a defunctionalization, similar to the already reported laser-induced defunctionalization of carbon nanotubes.[12] Here, the higher laser intensity and therefore a locally increased temperature results in the cleavage of the newly formed C–C bonds, reverting the sp^3 centers in the graphene lattice back to sp^2 configuration. A laser-induced defunctionalization is even more likely to occur in graphene due to the fact that the defunctionalization leads to a decrease of strain energy in the whole system. The concept of detaching functional moieties through laser or thermal treatment is widely utilized in the concept of the TG-MS characterization of covalently functionalized graphene samples[33] and in the annealing of

 © 2020 The Authors. Published by Wiley-VCH GmbH

graphene oxide[34] yielding a higher quality material with less defects.

In order to investigate the thermal stability of the graphene patterning, we carried out a temperature dependent Raman investigation to access insights into the reversibility of the covalent addend binding. Since the peroxide bond of DBPO can also be cleaved thermally upon heating, generating phenyl radicals, it has to be expected that a thermal heating of the wafer leads also to a parallel graphene functionalization up to a certain temperature threshold.[32] We started the measurements with a moderate temperature ramp of 5 °C per minute from 0 °C up to 125 °C (Figure 4a). Due to the low heating rate, it was possible to follow the temperature-based functionalization process by Raman spectroscopy. As illustrated by the respective optical images of the wafer (Figure S5) the DBPO film has vanished when a temperature of 100 °C was reached. For the investigation of the thermally-induced addend defunctionalization processes we increased the temperature ramp at 125 °C to 50 °C per minute, up to a final temperature of 450 °C.

Significantly, the D-band intensity at $\approx 1350\ cm^{-1}$ increased with increasing temperature to an I_D/I_G ratio of 2.0 at 50 °C. After 50 °C the D-band starts to decrease until 80 °C and increases again at 85 °C just to decrease once more at around 125 °C (Figure 4).

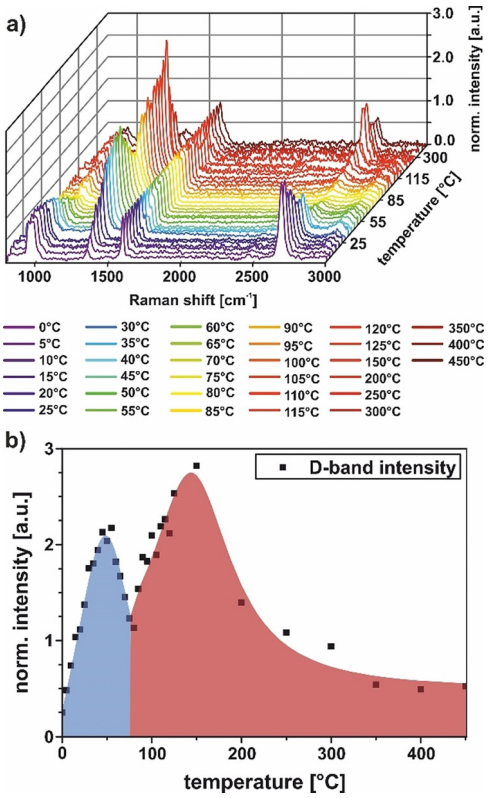

Figure 4. a) Temperature-dependent Raman measurement of monolayer Graphene coated with DBPO. b) Plot of D-band intensity evolution during functionalization (blue area) and defunctionalization (red area) over the temperature range from 0 °C to 450 °C, measured with a 532 nm laser, an integration time of 10 seconds, and an intensity of 0.88 mW.

The behavior of the D-band is similar to the observations made by Cançado et al.[35] where upon reaching a high functionalization degree the I_D/I_G ratio starts to decrease though further functionalization is occurring. This is attributed to the fact that the defect distance decreases below 3 nm, as disorder in the sp^2 system progresses. If two defects are closer than the average distance an electron-hole pair travels before scattering with a phonon, the contribution to the D-band will no longer add up independently, so the intensity of the D-band will decrease with respect to the G-band, although further functionalization is occurring. The increase of I_D/I_G ratio at 85 °C indicates an increase in inter defect distance, resulting in a return to the low functionalization regime. During this process, the system eventually reaches the low functionalization regime where upon further defunctionalization the D-band intensity decreases down to the values of intact graphene.

This behavior can also be nicely followed by the development of the 2D-band and D′-band intensities. The 2D-band development starts with a high I_{2D}/I_G ratio expected for monolayer graphene and constantly decreases during the functionalization process up to 85 °C due to the dampening effect of the functionalization. During the defunctionalization of the graphene monolayer, the I_{2D}/I_G ratio goes back almost to the initial value (Figure S6). For the D′-band an inverse trend is observed. It increases during the functionalization period and starts to decrease when approaching the defunctionalization regime (Figure S7). These studies show that thermal treatment of the 2D graphene architectures allows for controlling the degree of functionalization and can even lead to a restauration of an intact graphene lattice by erasing the chemical information stored during the preceding writing process (Scheme 2).

We now describe the imaging process of the laser induced 2D-functionalization of graphene. The laser writing as well as the read out of the stored 2D information is based on screening studies pointed out above. Therefore, a Raman map was designed, using the shape of "FAU". Each mapping point was irradiated with a 532 nm laser for 30 seconds applying a laser intensity of 1.6 mW. The successful patterning of chemical information concludes the "writing process". For the visualization of the imprinted pattern, as seen in Scheme 2, a "reading process" was established were a Raman map of the functionalized area is performed with a 633 nm laser—lower I_D/I_G contribution in the reading process (see Figure S8). The I_D/I_G ratios depicted and spatially resolved in Figure 5 provide excellent imaging of the chemical information of the 2D-patterned graphene. An average I_D/I_G ratio of 1.5 for the predefined functionalization spots is displayed, whilst the

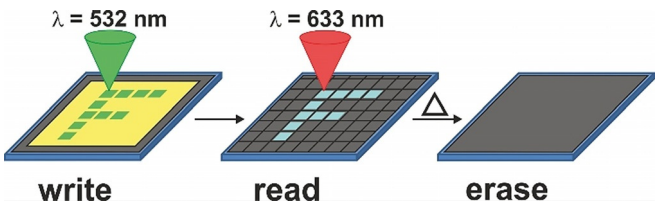

Scheme 2. Schematic illustration of the write/read/erase concept.

© 2020 The Authors. Published by Wiley-VCH GmbH

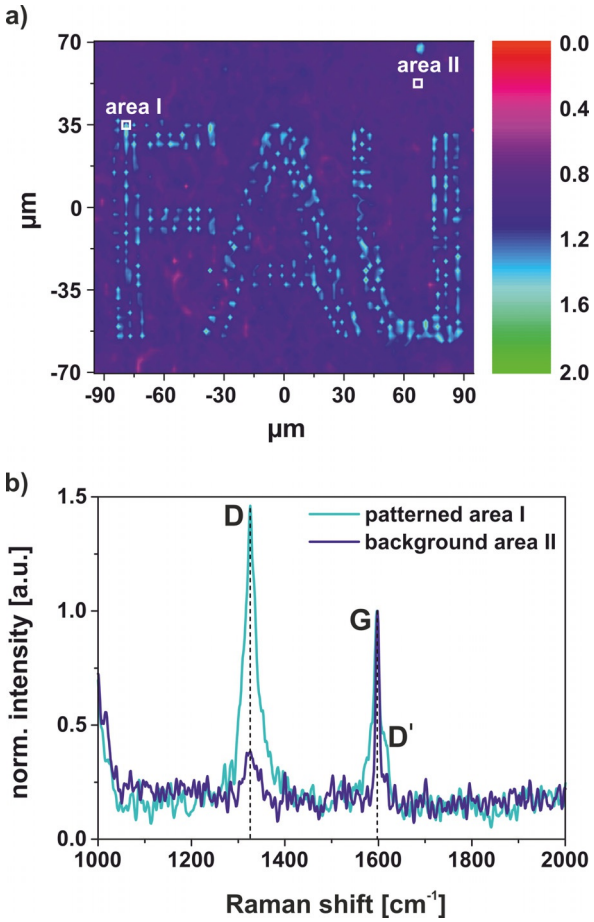

Figure 5. a) Raman map of 6912 measure points in a 186×144 µm area obtained by a 633 nm laser with an intensity of 1.6 mW (integration time: 8 s), showing the I_D/I_G ratios of the locally functionalized graphene, visualizing the predefined pattern. b) Raman point spectra obtained by the Raman map, of the patterned area I and the background area II normalized on the G-band.

unfunctionalized background and intact graphene region yields an I_D/I_G ratio between 0.4 and 0.9. By displaying the difference in I_D/I_G ratios between background and patterned area (Figure 5b), Raman measurements allow for visualization of the spatially resolved functionalization areas. One can observe a local introduction of sp^3 carbon centers at those points where irradiation by the 532 nm laser occurred. The resolution for differentiating between two patterning spots is approximately 2 µm and is limited by the spot size of the laser and the mesh of the "reading" map. Defined boundaries indicate the areas between the intact graphene lattice and the sp^3 regimes. With these "writing" and "reading" procedures we have realized 2D graphene-patterning by generating addend regions introducing areas of high functionalization. These take the shape of a desired pattern and an area of unfunctionalized graphene is left in the background. By thermal treatment, the chemical information stored on the graphene can be erased as shown by our temperature dependent Raman study (Figure 4a). This allows for the precise adjustment of the degree of functionalization, complete restauration of the graphene, and reusability for further storage of new chemical information.

Conclusion

We have introduced a very facile and efficient method for the covalent 2D-patterning of monolayer graphene via laser irradiation. We utilized the photo-cleavage of dibenzoylperoxide (DBPO) and optimized the subsequent radical additions to non-activated graphene up to a level where controlled covalent 2D-patterning of graphene initiated by spatially resolved laser writing is possible. Efficient covalent binding takes place exclusively on the laser illuminated areas. The visualization of the covalent addend patterning has been accomplished by scanning with a 633 nm laser and analyzing the corresponding I_D/I_G ratios in the spatially resolved Raman spectra. The covalent 2D-functionalization of graphene, which is monitored by scanning Raman microscopy (SRM) is completely reversible. This can be seen, for example, from stepwise heating causing controlled defunctionalization and eventually the complete restauration of the graphene sp^2 lattice. This new concept enables write/read/erase control over the covalent chemical information stored on the graphene surface. Moreover, by systematically varying the nature of covalent functionalities many types of programmable surface architectures can be generated opening a wide field of sophisticated applications. Investigations along these lines are currently under way in our laboratories examining other potential radical starters like AIBN and heteroatom marked DBPO as well as further 2D materials like MoS_2.

Acknowledgements

Funded by the Deutsche Forschungsgemeinschaft (DFG, German Research Foundation)—Project-ID 182849149—SFB 953. Open access funding enabled and organized by Projekt DEAL.

Conflict of interest

The authors declare no conflict of interest.

Keywords: covalent functionalization · covalent patterning · graphene · Raman spectroscopy · write/read/erase

[1] A. H. Castro Neto, F. Guinea, N. M. R. Peres, K. S. Novoselov, A. K. Geim, *Rev. Mod. Phys.* **2009**, *81*, 109–162.
[2] K. F. Mak, L. Ju, F. Wang, T. F. Heinz, *Solid State Commun.* **2012**, *152*, 1341–1349.
[3] K. S. Novoselov, A. K. Geim, S. V. Morozov, D. Jiang, Y. Zhang, S. V. Dubonos, I. V. Grigorieva, A. A. Firsov, *Science* **2004**, *306*, 666–669.
[4] A. Hirsch, J. M. Englert, F. Hauke, *Acc. Chem. Res.* **2013**, *46*, 87–96.
[5] J. Malig, A. W. I. Stephenson, P. Wagner, G. G. Wallace, D. L. Officer, D. M. Guldi, *Chem. Commun.* **2012**, *48*, 8745–8747.

 © 2020 The Authors. Published by Wiley-VCH GmbH

[6] J. Park, M. Yan, *Acc. Chem. Res.* **2013**, *46*, 181 – 189.
[7] J. L. Bahr, J. M. Tour, *Chem. Mater.* **2001**, *13*, 3823 – 3824.
[8] J. L. Bahr, J. Yang, D. V. Kosynkin, M. J. Bronikowski, R. E. Smalley, J. M. Tour, *J. Am. Chem. Soc.* **2001**, *123*, 6536 – 6542.
[9] E. A. Merritt, B. Olofsson, *Angew. Chem. Int. Ed.* **2009**, *48*, 9052 – 9070; *Angew. Chem.* **2009**, *121*, 9214 – 9234.
[10] J. Malmgren, S. Santoro, N. Jalalian, F. Himo, B. Olofsson, *Chem. Eur. J.* **2013**, *19*, 10334 – 10342.
[11] C. K. Chan, T. E. Beechem, T. Ohta, M. T. Brumbach, D. R. Wheeler, K. J. Stevenson, *J. Phys. Chem. C* **2013**, *117*, 12038 – 12044.
[12] F. Hof, R. A. Schäfer, C. Weiss, F. Hauke, A. Hirsch, *Chem. Eur. J.* **2014**, *20*, 16644 – 16651.
[13] R. Barthos, D. Méhn, A. Demortier, N. Pierard, Y. Morciaux, G. Demortier, A. Fonseca, J. B. Nagy, *Carbon* **2005**, *43*, 321 – 325.
[14] F. Liang, A. K. Sadana, A. Peera, J. Chattopadhyay, Z. Gu, R. H. Hauge, W. E. Billups, *Nano Lett.* **2004**, *4*, 1257 – 1260.
[15] P. Vecera, K. F. Edelthalhammer, F. Hauke, A. Hirsch, *Phys. Status Solidi B* **2014**, *251*, 2536 – 2540.
[16] A. Criado, M. Melchionna, S. Marchesan, M. Prato, *Angew. Chem. Int. Ed.* **2015**, *54*, 10734 – 10750; *Angew. Chem.* **2015**, *127*, 10882 – 10900.
[17] G. L. C. Paulus, Q. H. Wang, M. S. Strano, *Acc. Chem. Res.* **2013**, *46*, 160 – 170.
[18] J. M. Englert, K. C. Knirsch, C. Dotzer, B. Butz, F. Hauke, E. Spiecker, A. Hirsch, *Chem. Commun.* **2012**, *48*, 5025 – 5027.
[19] M. S. Dresselhaus, G. Dresselhaus, *Adv. Phys.* **1981**, *30*, 139 – 326.
[20] T. Enoki, M. Suzuki, M. Endo, in *Graphite intercalation compounds and applications*, Oxford University Press, New York, **2003**, pp. 9 – 10.
[21] J. C. Chacón-Torres, A. Y. Ganin, M. J. Rosseinsky, T. Pichler, *Phys. Rev. B* **2012**, *86*, 0754061 – 0754066.
[22] K. Amsharov, D. I. Sharapa, O. A. Vasilyev, M. Oliver, F. Hauke, A. Goerling, H. Soni, A. Hirsch, *Carbon* **2020**, *158*, 435 – 448.
[23] J. Holzwarth, K. Y. Amsharov, D. I. Sharapa, D. Reger, K. Roshchyna, D. Lungerich, N. Jux, F. Hauke, T. Clark, A. Hirsch, *Angew. Chem. Int. Ed.* **2017**, *56*, 12184 – 12190; *Angew. Chem.* **2017**, *129*, 12352 – 12358.
[24] J. Li, M. Li, L.-L. Zhou, S.-Y. Lang, H.-Y. Lu, D. Wang, C.-F. Chen, L.-J. Wan, *J. Am. Chem. Soc.* **2016**, *138*, 7448 – 7451.
[25] Z. Sun, C. L. Pint, D. C. Marcano, C. Zhang, J. Yao, G. Ruan, Z. Yan, Y. Zhu, R. H. Hauge, J. M. Tour, *Nat. Commun.* **2011**, *2*, 559.
[26] T. Wei, M. Kohring, M. Chen, S. Yang, H. B. Weber, F. Hauke, A. Hirsch, *Angew. Chem. Int. Ed.* **2020**, *59*, 5602 – 5606; *Angew. Chem.* **2020**, *132*, 5651 – 5655.
[27] L. Bao, B. Zhao, V. Lloret, M. Halik, F. Hauke, A. Hirsch, *Angew. Chem. Int. Ed.* **2020**, *59*, 6700 – 6705; *Angew. Chem.* **2020**, *132*, 6766 – 6771.
[28] H. Liu, S. Ryu, Z. Chen, M. L. Steigerwald, C. Nuckolls, L. E. Brus, *J. Am. Chem. Soc.* **2009**, *131*, 17099 – 17101.
[29] J. A. den Hollander, J. P. M. van der Ploeg, *Tetrahedron* **1976**, *32*, 2433 – 2436.
[30] K. Akihide, S. Hirochika, Y. Masayuki, T. Katsumi, *Bull. Chem. Soc. Jpn.* **1980**, *53*, 1393 – 1398.
[31] K. C. Knirsch, R. A. Schäfer, F. Hauke, A. Hirsch, *Angew. Chem.* **2016**, *128*, 5956 – 5960.
[32] G. Gao, D. Liu, S. Tang, C. Huang, M. He, Y. Guo, X. Sun, B. Gao, *Sci. Rep.* **2016**, *6*, 20034.
[33] R. A. Schäfer, D. Dasler, U. Mundloch, F. Hauke, A. Hirsch, *J. Am. Chem. Soc.* **2016**, *138*, 1647 – 1652.
[34] C.-M. Chen, J.-Q. Huang, Q. Zhang, W.-Z. Gong, Q.-H. Yang, M.-Z. Wang, Y.-G. Yang, *Carbon* **2012**, *50*, 659 – 667.
[35] L. G. Cançado, A. Jorio, E. H. M. Ferreira, F. Stavale, C. A. Achete, R. B. Capaz, M. V. O. Moutinho, A. Lombardo, T. S. Kulmala, A. C. Ferrari, *Nano Lett.* **2011**, *11*, 3190 – 3196.

Manuscript received: May 12, 2020
Accepted manuscript online: August 18, 2020
Version of record online: October 4, 2020

 © 2020 The Authors. Published by Wiley-VCH GmbH